Progress In Electromagnetics Research C, Vol. 55, 9–16, 2014

Dual Circularly Polarized Antenna with Suspended Strip Line Feeding

Jianjun Wu*, Hao Yang, and Yingzeng Yin

Abstract—A dual circularly polarized (CP) antenna is proposed in this paper. By employing suspended strip line to feed the patch at the two diagonal positions with 90° phase difference, single circular polarization is firstly obtained. Then dual circular polarization is excited by an L-shaped strip. The two feeding ports near the edges of the L-shaped strip arms provide the conversion between left-hand circular polarization (LHCP) and right-hand circular polarization (RHCP). Measured results show that the proposed antenna has 10-dB return loss bandwidth of 30.5% (2.08–2.83 GHz), 10-dB isolation bandwidth of 15.7% (2.29–2.68 GHz), 3-dB axial ratio (AR) bandwidth of 25.1% (2.16–2.78 GHz).

1. INTRODUCTION

Circularly polarized (CP) antennas can reduce multi-path interferences and allow flexible orientations between the transmitter and receiver. Therefore, CP antennas have been receiving increasing attention in communication applications such as satellite communication, Global Positioning System (GPS), radar tracking and radio frequency identification (RFID) readers. To broaden the axial ratio (AR) bandwidth of CP antennas, stacked structures with thick air substrates are often used [1, 2]. In [1], circular polarization is achieved by a corner truncated patch and a horizontally meandered strip is employed for good impedance matching. In [2], the patch is fed by four probes on a suspended microstrip feed line with sequential 90° phase delays.

In addition, CP antennas with diverse polarization senses can receive signals with left-hand circular polarization (LHCP) and right-hand circular polarization (RHCP) simultaneously. Antennas with CP diversity can significantly enhance channel capacity and numerous works on dual CP antennas have been reported [3–10]. However, the isolation solution between the LHCP and RHCP ports is still a challenging task. A branch-line coupler is used in [3] to obtain dual CP performance. In this design, a high port isolation of 25 dB is achieved by H-shaped slots etched on the ground. In [4], dual CP radiations are obtained by loading a T-shaped strip between two T-junction feed lines. Four metallic strips located at the slot corners are introduced to improve the port isolation. A novel dual CP antenna using even and odd feed-line modes is proposed in [5]. Good isolation with bandwidth of 87 MHz is achieved due to the different transmission line modes. Another common method to generate dual circular polarization is utilizing aperture-coupled microstrip feed line with two ports at the two ends of the feed line [6–10]. The phase delays to excite CP waves are generated from the coupling slots in the ground. Different polarization senses are determined by the currents flowing directions on the feed line. The dual CP antennas in [7, 8] act as rectifying antennas for wireless power transmission and energy harvesting. The isolation between the two ports is improved by adding a resistor on the split of round feed line in [9]. The design in [10] is a successful dual CP antenna with 10-dB isolation bandwidth of 19% and 3-dB AR bandwidth of 16%. It is explained in [10] that the feed line generates a quasi

Received 23 September 2014, Accepted 6 November 2014, Scheduled 10 November 2014

* Corresponding author: Jianjun Wu (jun542391752@126.com).

The authors are with the Science and Technology on Antenna and Microwave Laboratory, Xidian University, Xi'an, Shaanxi 710071, People's Republic of China.

travelling wave and the energy excited by one port has been coupled to the slots on the patch before arriving at the other port, which results in a high isolation.

In this paper, a dual CP antenna with an L-shaped suspended strip feed line is introduced. The L-shaped feed line has a similar operating mechanism to the aperture-coupled microstrip feed line in [9, 10]. The energy on the feed line is coupled to the patch directly by three probes instead of the coupling slots, and good port isolation can still be obtained simultaneously. The antenna structure is simple and easy to install, which is only composed of a ground plane and a square patch with a suspended strip feed line between them. Detailed designs of the proposed dual CP antenna are described in the following sections.

2. ANTENNA DESIGN

2.1. Design of Single CP Antennas

The antennas with suspended feed line are firstly designed for single circular polarization. Figure 1 shows the configurations of the CP antennas with different feeding port positions. The radiating patch is square and printed on a square Fr4 substrate with thickness of 1 mm, relative permittivity of 4.3 and dielectric loss tangent of 0.02. An air layer with height of 14 mm is used between the patch and the ground. Probes B and C locating at the patch diagonal connect the patch and the suspended feeding strip. In Figure 1(a), the inner core A of the SMA connector is located at the edge of the feeding strip (denoted as Antenna 1). While the probe A is between the two feeding probes in Figure 1(b) (denoted as Antenna 2). The probes A, B and C are of diameter of 0.65 mm and positioned along the center line of the microstrip feed line. The optimized parameters shown in Table 1 and the simulated results in the later sections are obtained with the aid of ANSYS HFSS 15 software.

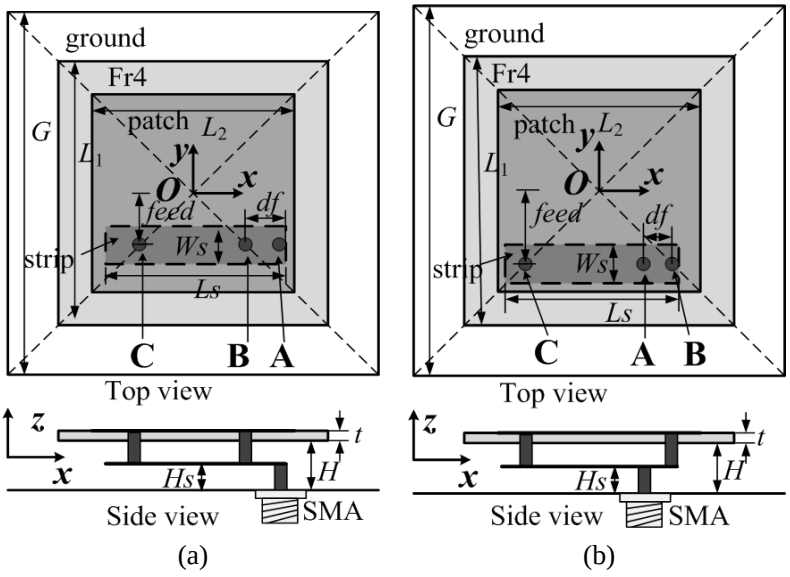

Figure 1. Configurations of the single CP antennas with suspended strip line feeding. (a) Antenna 1, and (b) Antenna 2.

Table 1. Detailed dimensions of the two single CP antennas and the dual CP antenna (unit: mm).

	G	L_1	L_2	H	H_s	t	$feed$	d_f	W_s	L_s
Antenna 1	100	70	48	14	5	1	14.5	5	12.5	39
Antenna 2	100	70	48	14	5	1	16	4	14	38
Dual CP antenna	100	70	48	14	5	1	17	6	12	40

In order to generate CP waves, two orthogonal modes with equal amplitude and 90° phase difference are needed. In our design, the mode along the patch diagonal can be yielded when either of the probes B and C is excited individually. Once the feeding port is excited, the currents flow along the strip line to probes B and C from probe A. The lengths of $|BC|$ in Figure 1(a) and $|AC| - |AB|$ in Figure 1(b) are about $0.25\lambda_0$ (λ_0 is the wavelength in free space corresponding to the center operating frequency), which can provide the required 90° phase difference on the probes B and C. Moreover, the other open-circuit end of the suspended strip line is extended to further tune the AR and input impedance. Figure 2 shows the simulated $|S_{11}|$ and AR of the two antennas with different feeding positions. Antenna 1 has a bandwidth of 30.1% (1.86–2.52 GHz) for $|S_{11}| < -10$ dB, 22.8% (2.06–2.59 GHz) for AR < 3 dB and an effective bandwidth of 20.1% (2.06–2.52 GHz) which is in gray color in Figure 2(a). Antenna 2 has a bandwidth of 24.7% (1.92–2.46 GHz) for $|S_{11}| < -10$ dB, 15.2% (2.13–2.48 GHz) for AR < 3 dB and an effective bandwidth of 14.4% (2.13–2.46 GHz). Figure 3 shows the simulated surface current distributions on the patch of Antenna 2 at different time frames. The equivalent direction of the currents is along the diagonal of the patch at $t = 0°$. While the current direction is along another diagonal at $t = 90°$. The currents rotate clockwise with time, which radiate LHCP in the bore-sight direction. Polarization of LHCP can be changed to RHCP when the feeding strip and probe A are mirrored with respect to yoz-plane.

Table 2 shows the comparisons of the profiles and bandwidths for the two antennas with single

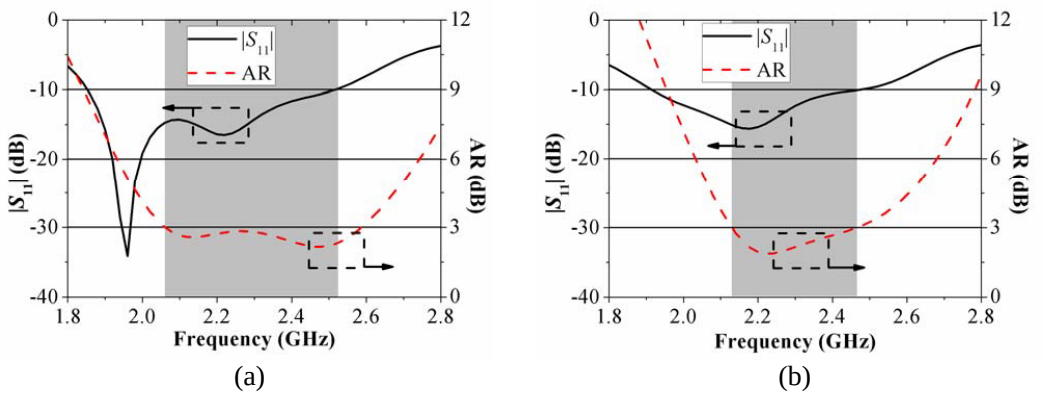

Figure 2. Simulated $|S_{11}|$ and AR of the two single CP antennas. (a) Antenna 1, and (b) Antenna 2.

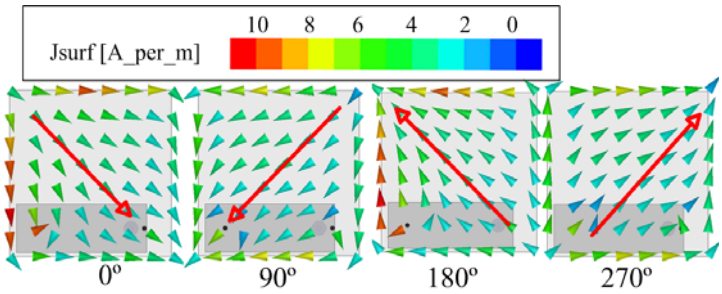

Figure 3. Simulated current distributions of Antenna 2 at 2.2 GHz.

Table 2. Comparisons of the single CP antennas to References [1, 2].

	Configuration	Height	Effective bandwidth
Ref. [1]	truncated patch fed by horizontally meandered strip	$0.14\lambda_0$	13.5%
Ref. [2]	sequential feed and stacked parasitic patch	$0.1\lambda_0$	16.4%
Antenna 1	single patch with suspended strip line feed	$0.12\lambda_0$	20.1%
Antenna 2		$0.12\lambda_0$	14.4%

circular polarization to the antennas in [1, 2]. The proposed antennas with similar antenna heights have wider effective bandwidths for $|S_{11}| < -10\,\text{dB}$ and AR $< 3\,\text{dB}$ than the referred ones. Moreover, the two referred antennas utilized at least three stacked substrates and the wide AR bands are partly due to the upper parasitic patches. But our antenna structure is simple with only one substrate. Compared to the design in [2], less metal probes are used in the proposed antenna which leads to a convenient fabricated procedure.

2.2. Design of Dual CP Antenna

Figure 4 shows the configuration of the proposed dual CP antenna. The suspended L-shaped feeding line consists of two strip lines described in the former section. The arm along x-axis of the L-shaped strip is for LHCP while the other arm along y-axis is for RHCP. Two probes are located at the ends of the strip, and another probe is at the corner of the strip. The proposed antenna structure is symmetrical with respective to phi = 45° plane. Therefore, the input impedances of the two ports are the same, and the radiation patterns are similar but with different polarization senses when either of the two ports is excited. Figure 5 depicts the surface current distributions on the L-shaped feeding strip when the LHCP port is excited. It can be seen that the energy flows upward and downward along the LHCP arm of the strip. The energy arrives at the upper probe at $t = 45°$ and at the corner probe at $t = 135°$ with a time delay of 90°. Some energy flows to the RHCP strip arm after $t = 90°$ and becomes attenuated.

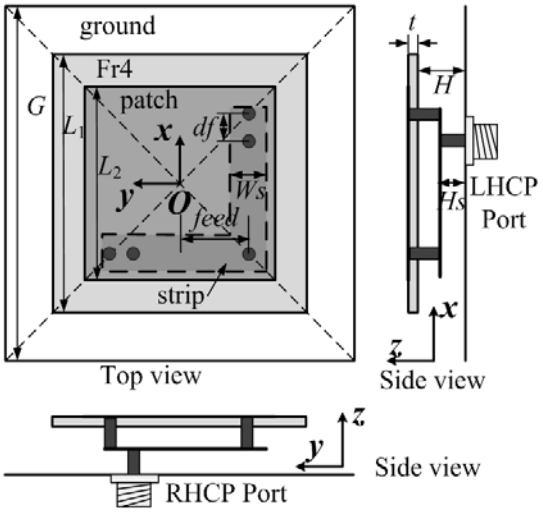

Figure 4. Configuration of the proposed dual CP antenna.

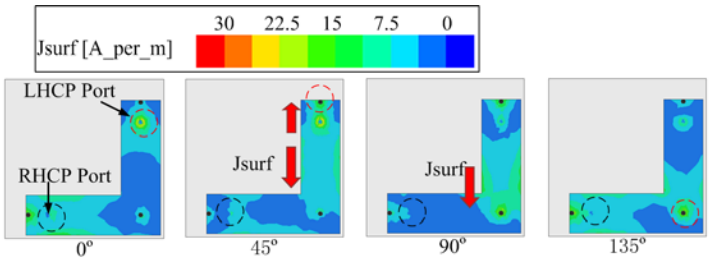

Figure 5. Simulated current distributions on the feeding strip.

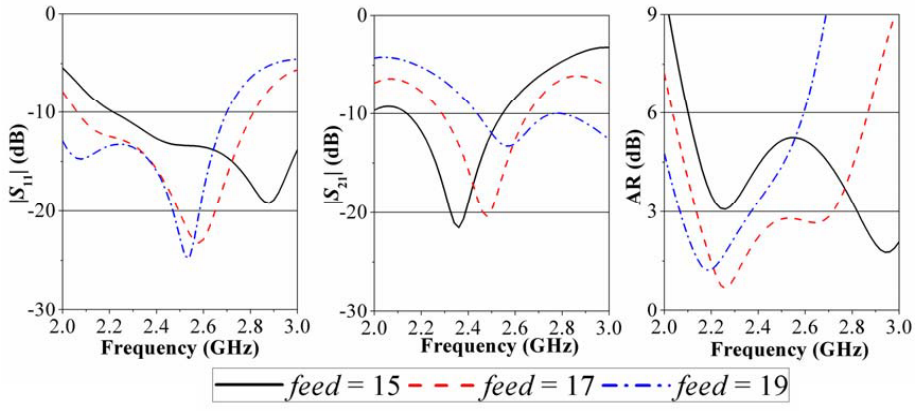

(a)

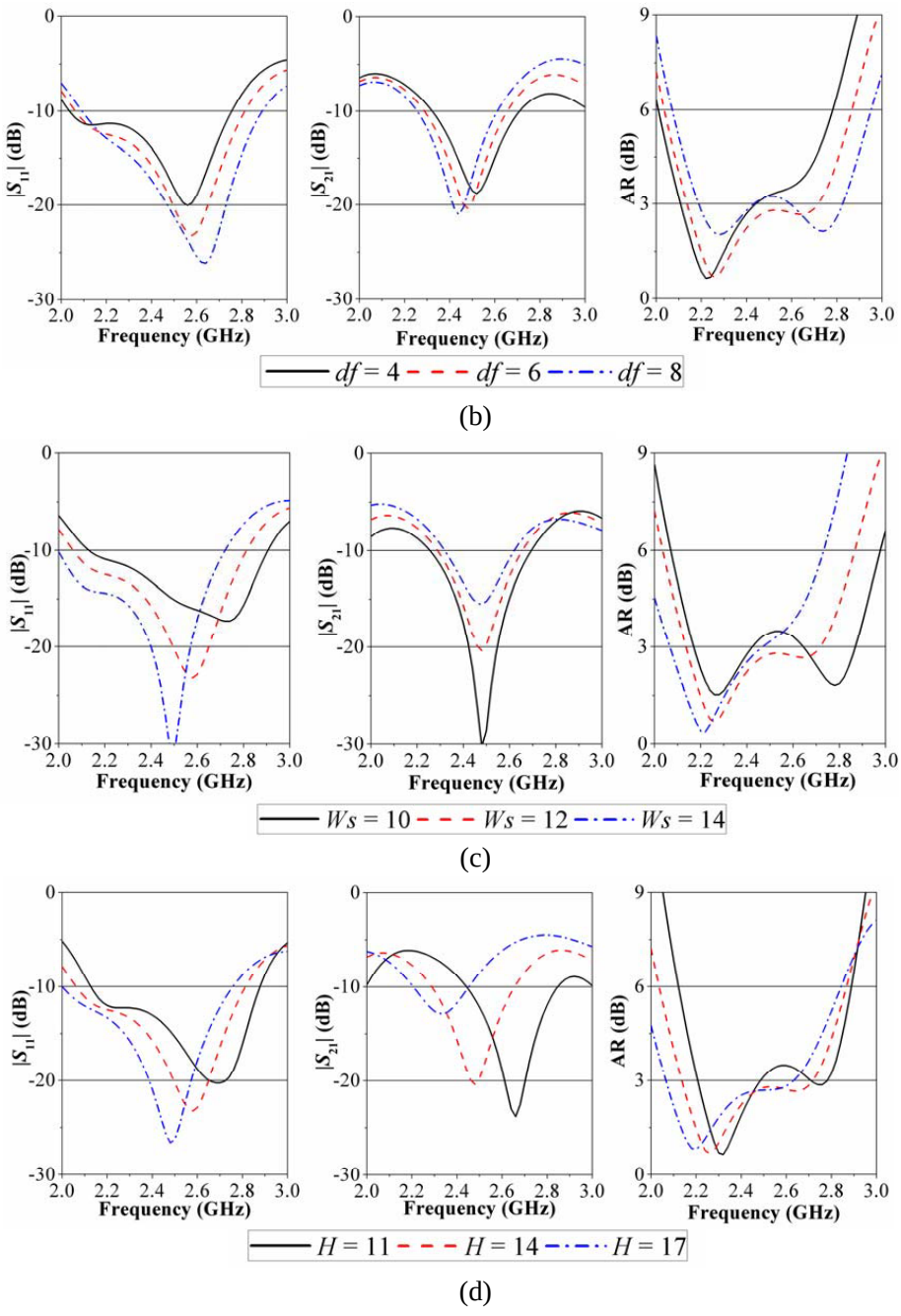

Figure 6. Effects of the key parameters on antenna performances: (a) *feed*, (b) d_f, (c) W_s, and (d) H.

The currents nearby the RHCP port are weak over the time domain. Good isolation between the LHCP and RHCP ports is obtained consequently.

Figure 6 illustrates the effects of the key parameters on the antenna performances. As shown in Figures 6(a) and (b), parameters *feed* and d_f have fierce influences on AR since the two parameters determine the phase difference between the feeding probes to generate circular polarization. As *feed* is increased, the minimum point of $|S_{11}|$ curve moves to lower frequency while the isolation $|S_{21}|$ becomes worse. Parameter d_f has an opposite effect on S parameters compared to *feed*. It is found from Figure 6(c) that the width of the strip W_s has a strong impact on the port isolation. Significant improvement of isolation $|S_{21}|$ is obtained with a decrease of W_s and the $|S_{11}|$ and AR curves move to

higher frequencies. It is to be noted that wider AR bandwidth can be achieved and the S parameters curves move to lower frequencies when antenna height H is increased, which can be seen in Figure 6(d). In the simulation procedure, the size of the radiating patch and the antenna height are firstly determined according to the required operating frequency, operating bandwidth and space limitation for the antenna installation. Then the length of the L-shaped strip and the positions of the feeding probes are tuned to achieve good CP performances. The width of the suspended strip is finally optimized to improve the port isolation and match the impedance of each port.

3. EXPERIMENTAL RESULTS

The proposed dual CP antenna prototype shown in Figure 7 was fabricated to validate the design strategies. S parameters were measured using Agilent N5062A Vector Network Analyzer. Radiation characteristics including AR, gain and radiation patterns were measured by a Satimo StarLab system. Since the LHCP and RHCP ports are symmetrical, the results for the excitation of LHCP port are given for brevity. Figure 8 shows the simulated and measured reflection coefficient and isolation of the proposed antenna. The measured bandwidth is 30.5% (2.08–2.83 GHz) for $|S_{11}| < -10$ dB and 15.7% (2.29–2.68 GHz) for $|S_{21}| < -10$ dB. High isolation better than 15 dB is obtained from 2.4 to 2.6 GHz. A small discrepancy between the simulated and measured results is due to the fabrication errors and the measurement loss. The measured AR and gain along $+z$-axis against frequency are shown in Figure 9. The measured 3-dB AR band is from 2.16 to 2.78 GHz (25.1%). Additionally, the antenna has a stable gain larger than 7 dBic over the effective band for isolation better than 10 dB. The measured normalized radiation patterns of the proposed antenna at 2.5 GHz is shown in Figure 10. The 3-dB AR beamwidths are 80° for xoz-plane and 30° for yoz-plane, and the front-to-back ratio is larger than 15 dB.

Table 3 tabulates the comparisons of the antenna sizes and performance between the proposed

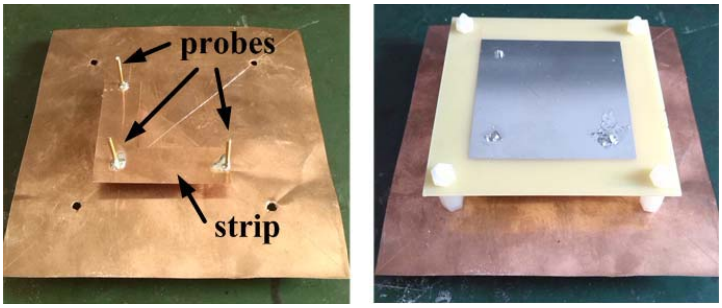

Figure 7. Photographs of fabricated antenna: (a) feeding structure and (b) top view.

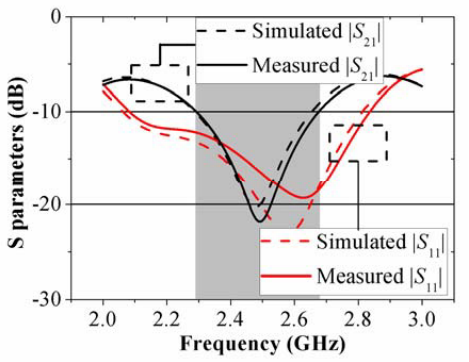

Figure 8. Simulated and measured S-parameters of the dual CP antenna.

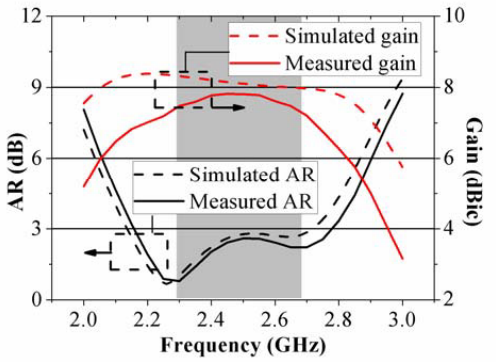

Figure 9. Simulated and measured AR and gain of the dual CP antenna fed by LHCP port.

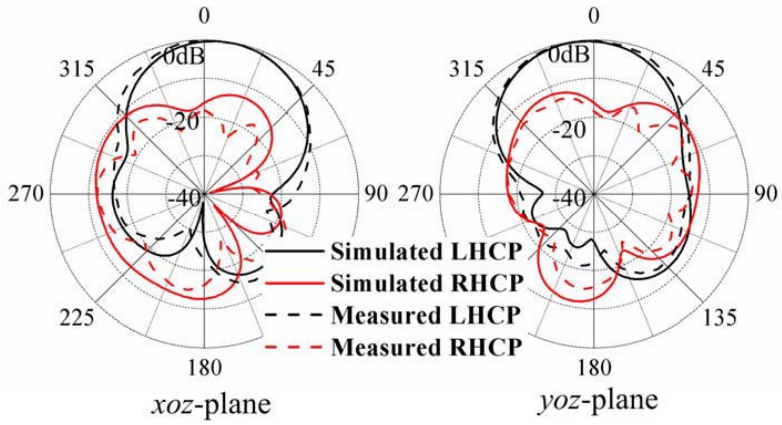

Figure 10. Simulated and measured normalized radiation patterns of the dual CP antenna fed by LHCP port at 2.5 GHz.

Table 3. Comparisons of the proposed antenna to the previous antennas.

	Configuration	Size ($\lambda_0 \times \lambda_0$)	Isolation	Effective bandwidth
[3]	branch-line coupler with H-shape slots	0.8×0.8	25 dB	16%
[4]	square slot, bidirectional radiation	0.58×1.1	25 dB	19%
[5]	patch with multi-mode feed	0.7×0.67	20 dB	3.2%
[9]	split-ring feed with a resistor	0.4×0.4	25 dB	4.3%
[10]	transmission line feed through slots	0.94×0.94	25 dB	16%
proposed	suspended strip line feed by probes	0.8×0.8	22 dB	15.7%

dual CP antenna and the antennas in references, in which λ_0 is the wavelength corresponding to the center operating frequency of each antenna, and the effective bandwidth refers to the band for return loss > 10 dB, isolation > 10 dB and AR < 3 dB. The proposed dual CP antenna is characterized by the following advantages: (1) The proposed antenna has a simple structure with easy feeding, though the size of the antenna is a little larger than the referred ones because a thick air layer is used. (2) High port isolation of 20 dB is obtained inherently. Other methods such as etching slot [3] and isolation resistor [9] are undesired. (3) The proposed antenna has a comparable effective bandwidth to the referred antennas. Besides, the antenna shows good radiation performances of wide AR bandwidth and high gain in the bore-sight direction.

4. CONCLUSION

A patch antenna fed by suspended strip line is proposed for dual circular polarization in this paper. Based on the L-shaped strip and probes feeding technology, good port impedance matching and isolation are obtained as well as good dual CP radiation characteristics. Experimental results verify that the optimized antenna has an effective bandwidth of 15.7% (2.29–2.68 GHz) for $|S_{11}| < -10$ dB, $|S_{21}| < -10$ dB, AR < 3 dB and gain > 7 dBic. Hence, the proposed dual CP antenna is a potential candidate for the applications requiring polarization diversity.

REFERENCES

1. Wang, Z. B., S. J. Fang, S. Q. Fu, and S. L. Jia, "Single-fed broadband circularly polarized stacked patch antenna with horizontally meandered strip for universal UHF RFID applications," *IEEE Transactions on Microwave Theory and Techniques*, Vol. 59, No. 4, 1066–1073, 2011.

2. Chen, Z. N., X. M. Qing, and H. L. Chung, "A universal UHF RFID reader antenna," *IEEE Transactions on Microwave Theory and Techniques*, Vol. 57, No. 5, 1275–1282, 2009.
3. Lai, X. Z., Z. M. Xie, Q. Q. Xie, and X. L. Cen, "A dual circularly polarized RFID reader antenna with wideband isolation," *IEEE Antennas Wireless Propagation Letters*, Vol. 12, 1630–1633, 2013.
4. Zhao, G., L. N. Chen, and Y. C. Jiao, "Design of a broadband dual circularly polarized square slot antenna," *Microwave and Optical Technology Letters*, vol. 50, No. 10, 2639–2642, 2008.
5. Narbudowicz, A., X. L. Bao, and M. J. Ammann, "Dual circularly-polarized patch antenna using even and odd feed-line modes," *IEEE Transactions on Antennas and Propagation*, Vol. 61, No. 9, 4828–4831, 2013.
6. Aloni, E. and R. Kastner, "Analysis of a dual circularly polarized microstrip antenna fed by crossed slots," *IEEE Transactions on Antennas and Propagation*, Vol. 42, No. 8, 1053–1058, 1994.
7. Harouni, Z., L. Cirio, L. Osman, A. Gharsallah, and O. Picon, "A dual circularly polarized 2.45-GHz rectenna for wireless power transmission," *IEEE Antennas Wireless Propagation Letters*, Vol. 10, 306–309, 2011.
8. Haboubi, W., H. Takhedmit, J.-D. Lan Sun Luk, S.-E. Adami, B. Allard, F. Costa, C. Vollaire, O. Picon, and L. Cirio, "An efficient dual-circularly polarized rectenna for RF energy harvesting in the 2.45 GHz ISM band," *Progress In Electromagnetics Research*, Vol. 148, 31–39, 2014.
9. Lai, X. Z., Z. M. Xie, and X. L. Cen, "Design of dual circularly polarized antenna with high isolation for RFID application," *Progress In Electromagnetics Research*, Vol. 139, 25–39, 2013.
10. Zhang, C. H., X. L. Liang, X. D. Bai, J. P. Geng, and R. H. Jin, "A broadband dual circularly polarized patch antenna with wide beamwidth," *IEEE Antennas Wireless Propagation Letters*, Vol. 13, 1457–1460, 2014.